Rheological Properties of a Semidilute Solution of Rodlike Macromolecules. 2. Transient Flows

John S. Dahler,* Sezar Fesciyan,† and Nicolas Xystris

Departments of Chemistry and Chemical Engineering, University of Minnesota, Minneapolis, Minnesota 55455. *Received December 14, 1982*

ABSTRACT: An investigation has been made of how semidilute solutions of rod polymers respond to suddenly imposed shear and extensional flows. The calculations are based on a modification of the classic Kirkwood–Riseman theory which incorporates the Doi–Edwards theory for the rotational diffusion coefficient appropriate to the semidilute regime as well as Freed and Edward's treatment of screened hydrodynamic interactions. The consequences of this screening are quantitatively assessed and so also are those of convective contributions to the polymer bead velocities, which become particularly important at high rates of shear and elongation.

Introduction

The theory used in this investigation has been described in an earlier paper,[1] henceforth referred to as I. It is a straightforward generalization to number concentrations in the *semidilute* regime, $L^{-3} \ll c \ll (dL^2)^{-1}$, of the Kirkwood–Riseman theory[2] of dilute solutions of rodlike molecules. Here, L and $d \ll L$, respectively, are the length and width of an individual rod.

The two most obvious consequences of increasing the polymer concentrations beyond the value L^{-3} are the inhibition of rotational diffusion and the screening of hydrodynamic interactions among the polymer molecules. According to Doi and Edwards,[3] the rotational diffusion coefficient appropriate to a *uniform* semidilute solution of rod polymers is related to the low-concentration limit, D_{r0}, in the manner $D_r \propto D_{r0}(cL^3)^{-2}$. Furthermore, because the tumbling motions of the molecules are influenced by the (averaged) orientations of their neighbors, one expects the rotational diffusion coefficient of a concentrated solution to be functionally dependent on the flow field. Although there appears to be no direct, experimental evidence in support of the latter assertion, light scattering measurements performed and analyzed by Zero and Pecora[4] have succeeded in confirming the former. Finally, Freed and Edwards[5] have shown that hydrodynamic screening can be taken into account by replacing the Oseen tensor of the original Kirkwood–Riseman theory with an effective, concentration-dependent tensor. These are the modifications of the dilute solution theory which have been incorporated into our treatment of the rheological behavior of semidilute rod polymer solutions.

In our previous paper we reported calculations of the viscosity and normal stress coefficients for steady-state homogeneous shear flows. These results were compared with those of Doi and Edwards[3] (DE) and of Jain and Cohen[6] (JC), the latter of which differed from ours only by their neglect of hydrodynamic screening whereas the former not only lacked this correction but also were based on an approximation to the stress tensor, which is invalid except at very low rates of shear. Here, we present calculations of the transient behavior that occurs in the early stages of a suddenly imposed homogeneous shear and investigate homogeneous elongational (extensional) flows as well.

The following section provides a summary of the theory. Applications of this theory to shear and extensional flows are given in the final section.

Description of the Theory

The stress tensor of a polymeric solution is given by the expression $\sigma = \sigma_S - c\sum_i \langle \vec{F}_i \vec{R}_i \rangle$. Here, σ_S is the contribution from the solvent (S), which we assume to be a Newtonian fluid with a shear viscosity coefficient η_S. c denotes the number concentration of the polymer molecules, each of which is modeled as a rod decorated with $N + 1$ beads evenly spaced at the positions $\vec{R}_i = A(i - N/2)\vec{u}$. $-\vec{F}_i$ is the (Stokes) force exerted on bead i by the surrounding solvent. The direction of the rod axis is denoted by the unit vector $\vec{u}$ and the bracket $\langle A \rangle$ indicates an average $\int d\vec{u}\, P(\vec{u},t)A$ over the associated orientational distribution function $P(\vec{u},t)$.

The bead contributions to the stress tensor are obtained by solving the (modified) Kirkwood–Riseman equations

$$\phi_{ij} + \zeta \sum_{k \neq i} \langle T_{ik} \rangle \phi_{kj} = f_{ij} \tag{1}$$

wherein

$$\phi_{ij} = -(2/N)^2(\zeta a^2 D_r)^{-1} \langle \vec{F}_i \vec{R}_j \rangle \tag{2}$$

and

$$f_{ij} = (2/N)^2(a^2 D_r)^{-1} \langle (\vec{V}_i^0 - d\vec{R}_i/dt)\vec{R}_j \rangle \tag{3}$$

Here, ζ is the bead friction coefficient and D_r the rotational diffusion coefficient of a rod polymer in the absence of flow. $\langle T_{ik} \rangle$ is the scalar-valued modulus of an effective, concentration- and flow-dependent hydrodynamic interaction tensor[5] which has been averaged over all possible orientations of the rodlike polymers, and $\vec{V}_i^0$ is the unperturbed solvent velocity at the position of bead i. Finally, the bead velocity $d\vec{R}_i/dt$ is given by the sum of convective and diffusive (Brownian) terms

$$d\vec{R}_i/dt = (\vec{V}_i^0 - \vec{u}\vec{u}\cdot\vec{V}_i^0) - D_r a(i - N/2)\ \mathrm{grad}_u \ln P \tag{4}$$

It is convenient to replace the discrete bead indices with continuous variables, $x = (2/N)(i - N/2)$, etc., and the matrices ϕ_{ij}, f_{ij}, and $\langle T_{ij} \rangle$ with the corresponding functions $\phi(x,y)$, $f(x,y)$, and $(2/N)(6\pi\eta_S a)^{-1}\hat{T}(x,y)$, respectively. Equation 1 then takes the form

$$\phi(x,y) + \lambda_0 \int_{-1}^{1} dz\, H(|x - z| - 2/N)\hat{T}(x,z)\phi(z,y) = f(x,y) \tag{5}$$

and the stress tensor becomes

$$\sigma = \sigma_S + (N/2)^3 c\zeta a^2 D_r \int_{-1}^{1} dx\, \phi(x,x) \tag{6}$$

$H(x)$ appearing in eq 5 is the unit step function and $\lambda_0 \equiv \zeta/6\pi\eta_S a \equiv b/a$, the so-called hydrodynamic strength parameter, equals the ratio of bead radius to segment length. Using Kirkwood's procedure for constructing approximate solutions of integral equations similar to (5), we obtain the expression

$$\phi(x,y) = \frac{1}{2}\sum_{-\infty}^{+\infty}(1 + \lambda_0 \hat{T}_p)^{-1} \int_{-1}^{1} dz\, f(z,y)\, \exp[i\pi p(x - z)] \tag{7}$$

†Present address: Department of Physics, Manhattan College, Bronx, NY 10471.

0024-9297/83/2216-1673$01.50/0

wherein

$$\hat{T}_p = \frac{1}{2}\int_{-1}^{1}dx\int_{-1}^{1}dz\ \hat{T}(x,z)\ \exp[i\pi p(z-x)] \quad (8)$$

According to the theory of Freed and Edwards,[5] these Fourier transforms of the hydrodynamic interaction satisfy the nonlinear integral equations

$$\hat{T}_p = (N/6)6\pi\eta_S a\int\frac{d^3k}{(2\pi)^3}\frac{g_p(k)-\tilde{g}_p(k)}{\eta_S k^2-\Sigma_0(k)} \quad (9a)$$

$$\Sigma_0(k) = -(Nc\zeta/4)\sum_{-\infty}^{+\infty}(1+\lambda_0 T_p)^{-1}g_p(k) \quad (9b)$$

with

$$g_p(k) = \int_{-1}^{1}dx\int_{-1}^{1}dy\ S_k(x,y)\ \exp[i\pi p(x-y)] \quad (10a)$$

$$\tilde{g}_p(k) = \int_{-1}^{1}dx\int_{-1}^{1}dy\ H(|x-y|-2/N)S_k(x,y)\ \exp[i\pi p(x-y)] \quad (10b)$$

and where

$$S_k(x,y) = \langle\exp(i\vec{k}\cdot\vec{u})(Na/2)(x-y)\rangle \quad (11)$$

Before these equations can be solved, the functions $S_k(x,y)$ must be evaluated and this, in turn, requires a knowledge of the orientational distribution function $P(\vec{u},t)$. This distribution function also is a necessary input to the computation of the driving forces $f(x,y)$ which appear in the formula (eq 7) for the tensor $\phi(x,y)$. We assume that $P(\vec{u},t)$ satisfies the continuity equation

$$\frac{\partial}{\partial t}P(\vec{u},t) + \mathrm{div}_u\ (\vec{u}P - \bar{D}_r\ \mathrm{grad}_u\ P) = 0 \quad (12)$$

and, along with Doi and Edwards,[3] suppose that the rods follow the motion of the solvent, the homogeneous flow field of which is given by $\vec{V}^0(\vec{r},t) = g(t)\cdot\vec{r}$. Accordingly, $d\vec{u}/dt = g\cdot\vec{u} - (\vec{u}\cdot g\cdot\vec{u})\vec{u}$. Finally, $\bar{D}_r$ is the orientation-averaged, concentration- and flow-dependent diffusion coefficient defined by Doi and Edwards:

$$\bar{D}_r^{-1/2} = D_r^{-1/2}\frac{4}{\pi}\int d\vec{u}\int d\vec{u}'\ P(\vec{u},t)P(\vec{u}',t)\ \sin(\vec{u}\vec{u}') \quad (13)$$

The theory is now complete. Once the flow field [$g = (\mathrm{grad}\ \vec{V}^0)^T$] has been selected, the continuity equation (12) can be solved for $P(\vec{u},t)$. This permits the calculation of the driving forces $f(x,y)$ and the structure functions $S_k(x,y)$, upon which the $g_p(k)$'s and $\tilde{g}_p(k)$'s are dependent; cf. eq 10. The integral equations (9) are then solved for the quantities $\hat{T}_p$. The next step is to calculate $\phi(x,y)$ from eq 7 and then, finally, the stress tensor is constructed according to eq 6.

Application to Shear Flow

The first example to be considered is the sample shear flow $\vec{V}^0(\vec{r},t) = g(t)\hat{e}_x\hat{e}_z\cdot\vec{r}$. Here, $g(t)$ denotes the homogeneous rate of shear and $\hat{e}_x$ and $\hat{e}_z$ are unit vectors parallel to the laboratory x and z axes, respectively. Among the observables associated with this flow are $\delta\eta = g^{-1}[\sigma_{xz} - (\sigma_S)_{xz}]$, the polymer contribution to the shear viscosity coefficient, and the two normal stress coefficients $\psi_1 = g^{-2}[\sigma_{zz} - \sigma_{xx}]$ and $\psi_2 = g^{-2}[\sigma_{yy} - \sigma_{zz}]$. From the theory of the preceding section we obtain for these coefficients the three formulas

$$\delta\eta = \frac{N^3c(\zeta a^2 D_r)}{12}\frac{1}{g}Y(\gamma)F(\gamma,c) \quad (14)$$

$$\psi_1 = \frac{N^3c(\zeta a^2 D_r)}{12}\frac{1}{g^2}Y_1(\gamma)F(\gamma,c) \quad (15)$$

$$\psi_2 = \frac{N^3c(\zeta a^2 D_r)}{12}\frac{1}{g^2}Y_2(\gamma)F(\gamma,c) \quad (16)$$

wherein $\gamma \equiv g/D_r$ is a dimensionless rate of shear.

The effects of hydrodynamic screening (the Freed–Edwards theory[5]) are confined to the multiplicative factor

$$F(\gamma,c) = \frac{6}{\pi^2}\sum_1^\infty\frac{1}{p^2}(1+\lambda_0\hat{T}_p)^{-1} \quad (17)$$

which equals unity when all of the moduli $\langle T_{ij}\rangle$ or $\hat{T}_p$ are negligibly small, that is, at very high polymer concentrations.

The three functions $Y(\gamma)$, $Y_1(\gamma)$, and $Y_2(\gamma)$ are related by the formulas $Y(\gamma) = 3\langle u_x u_z\rangle + \gamma\langle u_x^2 u_z^2\rangle$, $Y_1(\gamma) = 3\langle u_z^2 - u_x^2\rangle$, and $Y_2(\gamma) = 3\langle u_y^2 - u_z^2\rangle$ to orientational averages of quadratic and quartic functions of the direction cosines $u_\alpha = \vec{u}\cdot\hat{e}_\alpha$ ($\alpha = x, y, z$) of the rod axis. The origins of the quadratic and quartic terms are, respectively, the diffusive (Brownian) and convective contributions to the bead velocities; cf. eq 6.

The form of the continuity equation (12) appropriate to this flow field is[7]

$$\bar{D}_r^{-1}\frac{\partial P}{\partial t} + \bar{\gamma}\Gamma P = -(\hat{L}^2/\hbar^2)P \quad (18)$$

with $\bar{\gamma} \equiv g/\bar{D}_r$ and where

$$\hat{L}^2/\hbar^2 \equiv -\left[\csc\theta\frac{\partial}{\partial\theta}\left(\sin\theta\frac{\partial}{\partial\theta}\right) + \csc^2\theta\frac{\partial}{\partial\phi^2}\right]$$

and

$$\Gamma \equiv \cos^2\theta\cos\phi\frac{\partial}{\partial\theta} - \mathrm{ctn}\,\theta\sin\phi\frac{\partial}{\partial\theta} - 3\cos\theta\sin\theta\cos\phi$$

The solution of eq 18 can be expressed as the summation

$$P(\vec{u},t) = \sum_{l(\mathrm{even})}\sum_{m=0}^{l}b_{lm}(t)\mathcal{Y}_l^m(\vec{u}) \quad (19)$$

of the symmetry (parity) adapted spherical harmonics

$$\mathcal{Y}_l^m(\vec{u}) = Y_l^m(\vec{u}); \quad m = 0$$
$$= 2^{-1/2}[Y_l^m(\vec{u}) + (-)^m Y_l^{-m}(\vec{u})]; \quad 1 \le m \le l \quad (20)$$

For a flow which begins at time $t = 0$ and proceeds at a constant rate of shear, i.e., $g(t) = gH(t)$, the coefficients b_{lm} are governed by the coupled, ordinary differential equations

$$\frac{db_{lm}}{d\tau} = -X(\tau)l(l+1)b_{lm} - \gamma\sum_{l'm'}(lm|\Gamma|l'm')b_{l'm'} \quad (21)$$

Here, $\tau \equiv D_r t$ is a dimensionless time variable, $X(t) \equiv \bar{D}_r(t)/D_r$ is a functional of the entire set of coefficients $\{b_{lm}(t)\}$, and the $(lm|\Gamma|l'm')$ are matrix elements of Γ, which are easily evaluated.[3] The boundary condtions for (12) are $b_{lm}(0) = (4\pi)^{-1/2}\delta_{l0}\delta_{m0}$.

The functions $S_k(x,y)$, which must be known in order to compute the screening factor $F(\gamma,c)$, are related to the solutions of (21) by the formulas

$$S_k(x,y) = \sum_{n=0}^{\infty}(-)^n\{\pi^{1/2}b_{2n,0}(t)[2(4n+1)^{1/2}]\}j_{2n}(\tfrac{1}{2}kaN|x-y|) \quad (22)$$

with $j_l(x)$ denoting a spherical Bessel function. Similarly, for the orientational averages upon which the Y factors depend, $\langle u_x u_z\rangle = -(4\pi/15)^{1/2}b_{21}$, $\langle u_z^2 - u_x^2\rangle = -(4\pi/15)^{1/2}(b_{22} - 3^{1/2}b_{20})$, $\langle u_y^2 - u_z^2\rangle = -(4\pi/15)^{1/2}(b_{22} + 3^{1/2}b_{20})$,

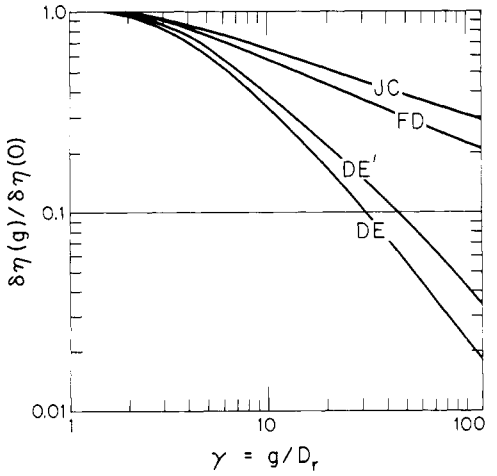

Figure 1. Shear viscosity increment, $\delta\eta(g)$, in units of the zero-shear rate limit, $\delta\eta(0)$, plotted vs. the dimensionless shear rate $\gamma = g/D_r$. The curve labelled DE′ is taken from ref 3. The others appeared in Figure 1 of ref 1, where it was shown that experimental data for PBLG in *m*-cresol agree quite well with the curve FD. The theories from which these curves were obtained are described in the text.

and $\langle u_x^2 u_z^2 \rangle$ is a linear combination of b_{00}, b_{20}, b_{22}, b_{40}, and b_{42}.[1,6] Finally, γ and $\bar{\gamma}$ are connected by $\gamma = \bar{\gamma}[Q(\bar{\gamma})]^{-2}$, with

$$Q(\bar{\gamma}) = 1 - 8\pi \sum_{n=1}^{\infty} \sum_{m=0}^{2n} \frac{2n-1}{2n+2} \left[\frac{(2n-3)!!}{(2n)!!} \right]^2 |b_{2n,m}(t)|^2 \quad (23)$$

Shear Flow Calculations

We previously have calculated steady-state values of the shear viscosity increment, $\delta\eta(g)$, in units of the zero-shear rate limit $\delta\eta(0)$.[1] Some of these results are reproduced here in Figure 1 to aid us in making comparisons between different theoretical estimates. Thus, the curve labeled FD (Fesciyan and Dahler) refers to values of $\delta\eta(g)/\delta\eta(0)$ computed directly from eq 14. The curve labeled JC agrees with results reported by Jain and Cohen[6] and has been obtained here (and in I) by setting the hydrodynamic screening factor $F(\gamma,c)$ equal to unity. The curve DE was computed by equating $F(\gamma,c)$ to unity and discarding the convective, quartic contribution to $Y(\gamma)$. This should have generated Doi and Edward's estimates of the shear viscosity coefficient, but it did not. The curve labeled DE′ is a plot taken directly from Doi and Edward's paper.

In Figure 2 we present values of the time-dependent shear viscosity coefficient, $\delta\eta(g,t)$, plotted in units of the corresponding steady-state limit, $\delta\eta(g,\infty) = \delta\eta(g)$. The abscissa values are of the dimensionless time $\tau = D_r t$. Separate plots are provided for five different values of the dimensionless shear rate $\gamma = g/D_r$, ranging from 0.1 to 50. For each of these there are curves labeled FD, DE, and KD. The first and second were computed in the manners just described in connection with Figure 1. The third was taken from the paper by Kuzuu and Doi.[7] The differences between the DE and KD curves of Figure 2 are analogous to those between the DE and DE′ curves of Figure 1. We believe these disparities are due to computational errors made by Doi and his co-workers.

Although the pairs of FD and KD curves in Figure 2 are rather similar, especially at high rates of shear, it should be borne in mind that the corresponding scale factors $[\delta\eta(g,\infty)]_{FD}$ and $[\delta\eta(g,\infty)]_{KD} = [\delta\eta(g)]_{DE}$ differ greatly; cf. the FD and DE′ curves of Figure 1. The fact that these differently scaled estimates of the viscosity coefficients (and those labeled DE as well) differ no more than they do is a consequence of the very similar time dependences of the $b_{lm}(t)$ coefficients that contribute to the quadratic and quartic terms of $Y(\gamma)$.

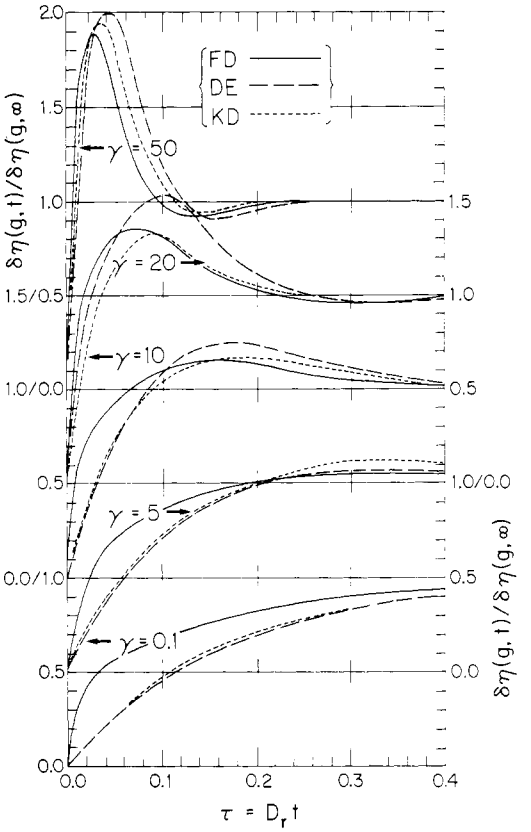

Figure 2. Time dependence of the shear viscosity increment $\delta\eta(g,t)$ for a uniform shear flow that begins at $t = 0$ and proceeds at a steady rate. Three curves are presented for each value of the (dimensionless) steady shear rate $\gamma = g/D_r$. The solid curves (labeled FD) were computed according to eq 14. The DE curves were obtained from eq 14 by neglecting hydrodynamic screening ($F = 1$) and discarding the convective (quartic in u_α) part of $Y(\gamma)$. The KD curves are taken from Figure 6 of ref 7.

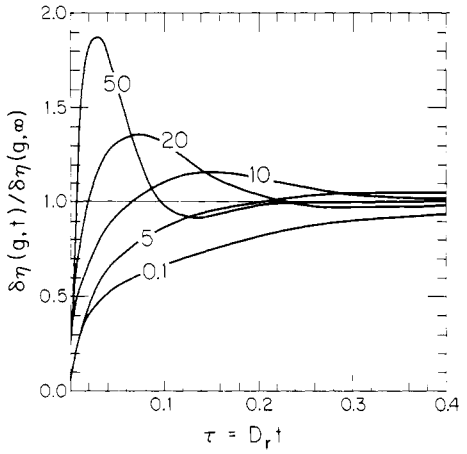

Figure 3. Time dependnece of $\delta\eta(g,t)$ according to the theory of this paper. This is a composite of the FD curves of Figure 2.

Figure 3 is a composite of the FD curves from Figure 2. It is directly comparable and strikingly similar to Figure 6 of Kuzuu and Doi.

Shown in Figures 4 and 5 are the variations with time of the first and second normal stress coefficients, ψ_1 and ψ_2, respectively. The shear rate dependencies of the steady-state limits of these coefficients were reported in I and were compared there with estimates (labeled DE in Figure 1 of I) obtained by ignoring the effects of hydrodynamic interactions. Our present values of ψ_1 and ψ_2 differ from those reported by Kuzuu and Doi (their Figures 8 and 9) for two reasons: (i) their $b_{lm}(t)$ coefficients ap-

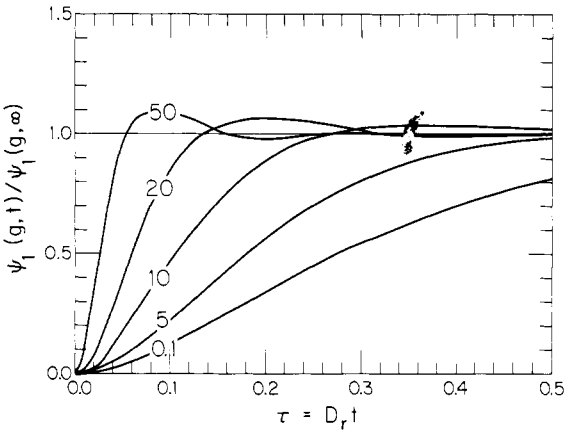

Figure 4. Time dependence of the first normal stress coefficient, $\psi_1(g,t)$, for the same shear flow described in the caption of Figure 2. The steady-state, long-time limits of this coefficient were shown in Figure 1 of ref 1.

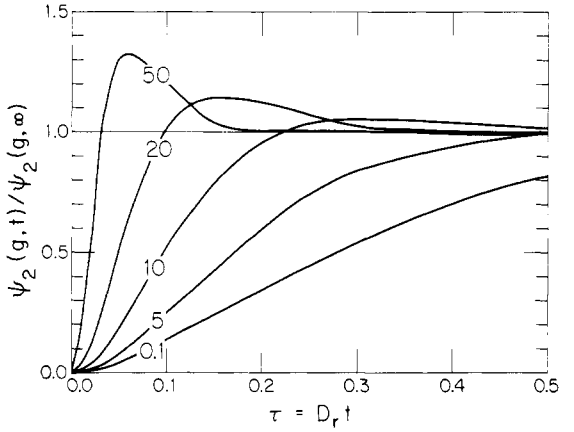

Figure 5. Time dependence of the second normal stress coefficient, $\psi_2(g,t)$.

parently are different from ours and (ii) our results incorporate the screening corrections which theirs do not. Despite these differences our results and Kuzuu and Doi's are qualitatively alike.

Application to Extensional Flow

Here the flow field is $\vec{V}^0(\vec{r},t) = \dot{\epsilon}(t)(\hat{e}_z\hat{e}_z - {}^1/_2\hat{e}_x\hat{e}_x - {}^1/_2\hat{e}_y\hat{e}_y)\cdot\vec{r}$, with $\dot{\epsilon}(t)$ equal to the homogeneous rate of extension. The sole observable we consider is the Trouton viscosity

$$\eta_{Tr} = \frac{\sigma_{zz} - \sigma_{xx}}{\dot{\epsilon}} = \frac{N^3c(\zeta a^2 D_r)}{12}\frac{1}{\dot{\epsilon}}Y_{Ex}(\alpha)F(\alpha,c) \quad (24)$$

with $\alpha = 3\dot{\epsilon}/2D_r$ and where $F(\alpha,c)$ is the hydrodynamic screening factor defined by eq 17. The driving force $Y_{Ex}(\alpha)$ is equal to the sum ${}^3/_2(3\langle u_z{}^2\rangle - 1) + {}^2/_3\alpha\langle(u_z{}^2 - {}^1/_2u_x{}^2 - {}^1/_2u_y{}^2)(u_z{}^2 - u_x{}^2)\rangle$ of diffusive and convective contributions.

The configurational continuity equation appropriate to this (z) axially symmetric flow is[7]

$$\frac{\partial P}{\partial t} = \bar{D}_r\frac{\partial}{\partial\mu}\left[(1-\mu^2)\left(\frac{\partial P}{\partial\mu} - \bar{\alpha}\mu P\right)\right] \quad (25)$$

with $\mu \equiv \vec{u}\cdot\hat{e}_z = \cos\theta$ and $\bar{\alpha} = 3\dot{\epsilon}/2\bar{D}_r$. Its solution

$$P(\vec{u},t) = \sum_{l=0}^{\infty}(4\pi)^{-1}a_l(t)P_l(\mu) \quad (26)$$

can be expanded in terms of Legendre polynomials $P_l(\mu)$ with coefficients $a_l(t)$ which satisfy the coupled, ordinary differential equations

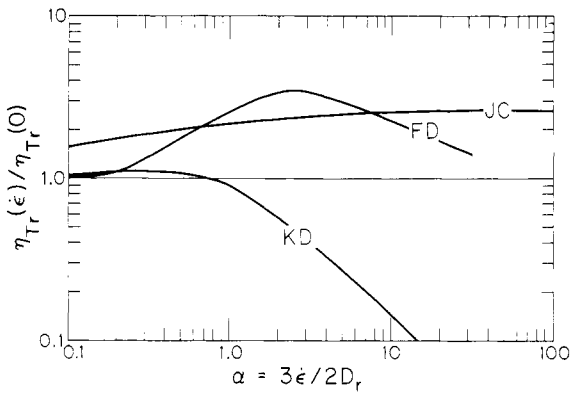

Figure 6. Dependence of the Trouton viscosity coefficient on the dimensionless rate of extension, $\alpha = 3\dot{\epsilon}/2D_r$. The curve labeled KD was taken from Figure 2 of ref 7. The FD curve, calculated according to eq 24, is unreliable for $\alpha \gtrsim 3$. The JC curve is a plot of eq 24 with $F(\gamma,c)$ set equal to unity.

$$\frac{da_l}{dt} = -D_r\alpha(t)l(l+1)\left[\left\{\frac{1}{\bar{\alpha}(t)} - \frac{1}{(2l+3)(2l-1)}\right\}a_l + \frac{l+2}{(2l+5)(2l+3)}a_{l+2} - \frac{l-1}{(2l-3)(2l-1)}a_{l-2}\right] \quad (27)$$

We consider the special case of $\dot{\epsilon}(t) = \dot{\epsilon}H(t)$. The corresponding initial conditions are $a_l(0) = \delta_{l0}$.

The functions $S_k(x,y)$ and the orientational averages that contribute to $Y_{Ex}(\alpha)$ are related to the expansion coefficients as follows:

$$S_k(x,y) = \sum_{n=0}^{\infty}(-)^n a_{2n}(t)j_{2n}\left(\frac{1}{2}kaN|x-y|\right) \quad (28)$$

$$\langle u_z{}^2\rangle = \frac{1}{3}\left(\frac{2}{3}a_2 + a_0\right) \quad (29a)$$

$$\left\langle\left(u_z{}^2 - \frac{1}{2}u_x{}^2 - \frac{1}{2}u_y{}^2\right)(u_z{}^2 - u_y{}^2)\right\rangle = \left\langle u_z{}^4 - 2u_z{}^2u_x{}^2 + \frac{2}{3}u_x{}^4\right\rangle = \frac{1}{35\times 54}(100a_4 + 72a_2 + 315a_0) \quad (29b)$$

and the connection between α and $\bar{\alpha}$ is $\alpha = \bar{\alpha}[Q(\bar{\alpha})]^{-2}$, with

$$Q(\bar{\alpha}) = 1 - 2\sum_{n=1}^{\infty}\frac{2n-1}{(2n+2)(4n+1)}\left[\frac{(2n-3)!!}{(2n)!!}\right]|a_{2n}(t)|^2 \quad (30)$$

Extensional Flow Calculations

The extension rate dependence of the steady-state Trouton coefficient $\eta_{Tr}(\dot{\epsilon})$ is shown in Figure 6, where it is plotted, in units of $\eta_{Tr}(0)$, vs. $\alpha = 3\dot{\epsilon}/2D_r$. Curve FD, which has been computed according to eq 24, is unreliable for values of α in excess of 3. When α increases beyond this limit so many expansion coefficients $a_l(t)$ make significant contributions to the functions $S_k(x,y)$—as well as to $g_p(k)$, $\tilde{g}_p(k)$, and $\hat{T}_p$—that an accurate evaluation of $F(\alpha,c)$ becomes prohibitively expensive. This is a reflection of the fact that the Legendre polynomial expansion (26) of $P(\vec{u},t)$ converges very slowly for large values of α. Although this has not hampered our ability to generate accurate estimates of the few low-order expansion coefficients (cf. eq 29) that contribute to the driving force $Y_{Ex}(\alpha)$, it does greatly complicate calculation of the hydrodynamic screening factor.

The curve labeled KD has been taken directly from the paper by Kuzuu and Doi.[7] Identical results are obtained from eq 24 by setting the factor $F(\alpha,c)$ equal to unity and

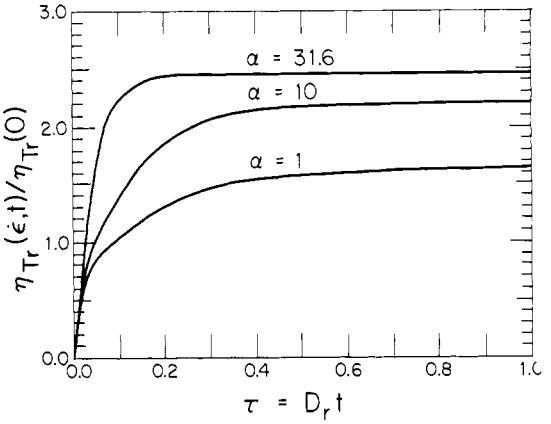

Figure 7. Time dependence of the Trouton viscosity, in units of its steady-state value for a zero rate of extension. The flow begins at time $t = 0$ and proceeds thereafter with a constant rate of extension.

discarding the convective, quartic contribution to $Y_{Ex}(\alpha)$. The third curve in Figure 6 has been labled JC because it is related to our general formula (24) in the same way that Jain and Cohen's shear viscosity increment $\delta\eta$ is related to our formula (14). Thus, the JC curve of Figure 6 was computed from (24) by setting the hydrodynamic screening factor F equal to unity. The noteworthy feature is the immense importance to the Trouton viscosity of the convective driving force that was neglected by Kuzuu and Doi. It is this alone which is responsible for the enormous difference between the JC and KD curves of Figure 6, a difference which is directly comparable to that between the curves JC and DE of Figure 1.

Kuzuu and Doi presented plots of the time-dependent Trouton viscosity $\eta_{Tr}(\dot{\epsilon},t)$ for the three values 1, 10, and 31.6 of the dimensionless rate of extension $\alpha = 3\dot{\epsilon}/2D_r$. From the KD curves of Figure 6 we see that the values of $\mathcal{R}_{KD}(\alpha) \equiv [\eta_{Tr}(\dot{\epsilon})/\eta_{Tr}(0)]_{KD}$ which correspond to these three homogeneous rates of extension are ordered as follows: $\mathcal{R}_{KD}(1) > \mathcal{R}_{KD}(10) > \mathcal{R}_{KD}(31.6)$. However, according to the JC approximation this ordering is reversed, viz., $\mathcal{R}_{JC}(1) < \mathcal{R}_{JC}(10) < \mathcal{R}_{JC}(31.6)$. It is this which accounts for the totally different arrangement of the three (JC) curves in our Figure 7 and those appearing in the comparable Figure 2 of Kuzuu and Doi's paper.

Acknowledgment. We acknowledge the support of the National Science Foundation and the donors of the Petroleum Research Fund, administered by the American Chemical Society.

References and Notes

(1) Fesciyan, S.; Dahler, J. S. *Macromolecules* **1982**, *15*, 517.
(2) Riseman, J.; Kirkwood, J. G. *J. Chem. Phys.* **1950**, *18*, 572. Kirkwood, J. G.; Auer, P. L. *Ibid.* **1951**, *19*, 281. Kirkwood, J. G.; Plock, R. J. *Ibid.* **1956**, *24*, 665. These papers also can be found in the book: "Macromolecules, J. G. Kirkwood Collected Works"; Gordon and Breach: New York, 1967.
(3) Doi, M.; Edwards, S. F. *J. Chem. Soc., Faraday Trans. 2* **1978**, *74*, 560, 918.
(4) Zero, K. M.; Pecora, R. *Macromolecules* **1982**, *15*, 87.
(5) Freed, K. F. In "Progress in Liquid Physics"; Croxton, C. A., Ed.; Wiley: New York, 1978.
(6) Jain, S.; Cohen, C. *Macromolecules* **1981**, *14*, 759.
(7) Kuzuu, N. Y.; Doi, M. *Polym. J.* **1980**, *12*, 883.

Notes

Synthesis of Methacrylate and Acrylate Monomers of Cholesteric Esters via Phase-Transfer Catalysis

PAUL J. SHANNON

Armstrong World Industries, Inc., Research and Development, Lancaster, Pennsylvania 17604.
Received January 27, 1983

We have been interested in the synthesis and properties of polymeric liquid crystals that have liquid crystalline moieties connected to the main polymer chain by flexible spacer groups as originally described by Ringsdorf et al.[1] The synthesis of polymethacrylates and polyacrylates of this type requires the formation of monomers such as **3** (Scheme I), which have a mesogen (in this case, the cholesteric ester) connected to the methacrylate moiety by a flexible methylene chain. Although monomers containing such functionality have been synthesized,[2-5] the acylation methods used in their preparation require chromatographic purification of the products and give only modest yields of the desired monomers. We describe here a new two-step approach to methacrylate and acrylate monomers of type **3**, which involves no chromatography and gives high overall yields (Scheme I).[6]

Results and Discussion

The efficient synthesis of monomers **3** relies upon insertion of the polymerizable moiety in the last step by displacement of bromide ion from ω-bromo esters **2** with potassium methacrylate or potassium acrylate. The substitution reaction can be performed in dimethylformamide solvent or by use of appropriate phase-transfer conditions. Although displacement of bromide ion by acetate anion under phase-transfer conditions is well-known,[7,8] the use of methacrylate or acrylate salts for such reactions has not received much attention.[9]

Scheme I

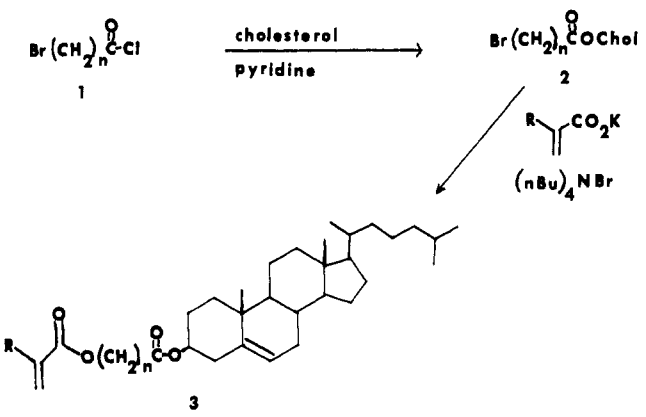

The requisite cholesteryl ω-bromoalkyl esters **2** are conveniently prepared by acylation of cholesterol in ethanol-free chloroform or ether–dichloromethane (4:1) with ω-bromoalkyl acid chlorides. The cholesteric esters **2** are heated to reflux in water–chloroform solvent with an excess of acrylate or methacrylate potassium salt, a catalytic amount of tetra-*n*-butylammonium bromide phase-transfer reagent, and ionol, a radical inhibitor. Alternatively, dimethylformamide can be used in place of the biphasic solution and phase-transfer reagent. Our experience indicates that although dimethylformamide provides a higher rate of reaction, the phase-transfer conditions result in a higher yield in product. In either case the monomers can be readily purified by recrystallization. Yields, phase transitions, and spectroscopic data for the monomers and ω-bromoalkyl esters we have prepared are listed in Table I.

It should be noted that several of these monomers have

0024-9297/83/2216-1677$01.50/0